# An amended Ehrenfest theorem for the Gross-Pitaevskii equation in one- and two-dimensional potential boxes

Hidetsugu Sakaguchi<sup>1</sup> and Boris A. Malomed<sup>2,3</sup>

<sup>1</sup>Department of Applied Science for Electronics and Materials,
Interdisciplinary Graduate School of Engineering Sciences,
Kyushu University, Kasuga, Fukuoka 816-8580, Japan

<sup>2</sup>Department of Physical Electronics, School of Electrical Engineering,
Faculty of Engineering, and Center for Light-Matter Interaction,
Tel Aviv University, P.O. Box 39040 Tel Aviv, Israel and

<sup>3</sup>Instituto de Alta Investigación, Universidad de Tarapacá, Casilla 7D, Arica, Chile

It is known that the usual form of the Ehrenfest theorem (ET), which couples the motion of the center of mass (COM) of the one-dimensional (1D) wave function to the respective classical equation of motion, is not valid in the case of the potential box, confined by the zero boundary conditions. A modified form of the ET was proposed for this case, which includes an effective force originating from the interaction of the 1D quantum particle with the box' edges. In this work, we derive an amended ET for the Gross-Pitaevskii equation (GPE), which includes the cubic nonlinear term, as well as for the 2D square-shaped potential box. In the latter case, we derive an amended COM equation of motion with an effective force exerted by edges of the rectangular box, while the nonlinear term makes no direct contribution to the 1D and 2D versions of the ET. Nonetheless, the nonlinearity affects the amended ET through the edge-generated force. As a result, the nonlinearity of the underlying GPE can make the COM motion in the potential box irregular. The validity of the amended ET for the 1D and 2D GPEs with the respective potential boxes is confirmed by the comparison of numerical simulations of the underlying GPE and the corresponding amended COM equation of motion. The reported findings are relevant to the ongoing experiments carried out for atomic Bose-Einstein condensates trapped in the box potentials.

#### I. INTRODUCTION

The Ehrenfest theorem (ET), known since 1927 [1, 2], is the fundamental tenet of quantum mechanics, which states that the center of mass (COM) of a wave packet moves according to the respective classical Newton's equation, in which the role of the potential force is played by its quantum-mechanical expectation value [3–5]. On the other hand, it was found that the ET in its canonical form does not apply to the one-dimensional (1D) quantum-mechanical setting including an infinitely deep potential box [6–9] (see also a general discussion of the applicability of the ET in Ref. [10]). Indeed, the formal application of the ET to the particle in the box obviously predicts that the COM of any wave packet must perform shuttle motion with a constant velocity, as no force acts upon the particle inside the box. However, this is not true, as the analytical solution of the corresponding Schrödinger equation readily produces exact wave functions which feature time-periodic motion of the COM with variable acceleration (see, e.g., Eq. (16) and Fig. 3(b) below). A qualitative explanation to this effect, which, in principle, may be considered as an example of the phenomenology of quantum anomalies" [11–17], is provided by effective forces exerted over the quantum particle by the walls (edges) of the 1D potential box. Taking these forces into account makes it possible to amend the ET, validating it for the quantum particle trapped in the 1D potential box [8, 9],

To the best of our knowledge, the modification of the ET for quantum particles in a two-dimensional (2D) infinitely deep potential box of the square shape was not previously reported. This setup is made experimentally relevant by the realization of optical boxes trapping atomic Bose-Einstein condensates (BECs) [21] [18–21] (see also a theoretical work [22]). Furthermore, the experimentally reported trapping of atomic Bose-Einstein condensates suggests to extend the ET for the nonlinear Gross-Pitaevskii equation (GPE), instead of the linear single-particle Schrödinger equation. The subject of the present work is the derivation of the extended (amended) ET for the 2D and 1D GPEs with the self-attractive or repulsive cubic nonlinearity, which are subject to the zero (Dirichlet) boundary conditions (BC) representing the 2D or 1D potential boxes. The amended ET for the 2D and 1D versions of the GPE is derived in Section 2. Basic analytical and numerical solutions, which corroborate and illustrate the amended ET in both the 2D and 1D cases, are produced, in a concentrated form, in Section 3. The paper is concluded by Section 4.

#### II. THE AMENDED ET FOR THE 2D AND 1D POTENTIAL BOXES

The 2D GPE for the mean-field wave function  $\psi(x,y,t)$  is written, in the scaled notation, as

$$i\frac{\partial\psi}{\partial t} = -\frac{1}{2}\nabla^2\psi + U(x,y)\psi + g|\psi|^2\psi \tag{1}$$

[12], where U(x,y) is the trapping potential, while g=-1 or +1 corresponds to the self-attraction or repulsion, respectively. When g=0, Eq. (1) reduces to the linear Schrödinger equation. The infinitely deep potential box is represented by the Dirichlet BC at edges of the square-shaped area (rectangular box) of size L, i.e.,

$$\psi(x = \pm L/2, |y| \le L/2) = \psi(y = \pm L/2, |x| \le L/2) = 0,$$
(2)

while the smooth potential is absent inside the box, i.e. U = 0. If these BC are adopted, the solution to Eq. (1) is considered only inside the square. The 1D version of the model is produced by the reduction of Eqs. (1) and (2) to the single coordinate x, as shown below.

To derive the ET, we define the COM coordinates,  $\mathbf{R} = (X, Y)$ , as

$$X = \frac{1}{N} \iint x \left| \psi(x, y) \right|^2 dx dy, \ Y = \frac{1}{N} \iint y \left| \psi(x, y) \right|^2 dx dy \tag{3}$$

where  $N = \int \int |\psi|^2 dx dy$  is the norm of the mean-field wave function, which is proportional to the number atoms in BEC. If the GPE is subject to the zero BC (2), the integration in Eq. (3) is constrained to the inner area of the potential box.

First, we derive an expression for the COM velocity,  $d\mathbf{R}/dt$ , differentiating expression (3) and substituting  $\partial \psi/\partial t$  as per Eq. (1):

$$\frac{d\mathbf{R}}{dt} = \frac{1}{N} \int \int \mathbf{r} \left( \frac{i}{2} \psi^* \nabla^2 \psi + \text{c.c.} \right) dx dy, \tag{4}$$

where  $\mathbf{r} = (x, y)$ , with both \* and c.c. standing for the complex conjugate (the terms  $\sim U$  and  $\sim g$  immediately cancel out in Eq. (4)). Further, expression (4) can be transformed by means of the integration by parts, using the following identity in the integrand:

$$ix_{j}\psi^{*}\partial_{kk}^{2}\psi + \text{c.c.} \equiv \left[i\partial_{k}\left(x_{j}\psi^{*}\partial_{k}\psi\right) - ix_{j}\left|\partial_{k}\psi\right|^{2} - i\psi^{*}\partial_{j}\psi\right] + \text{c.c.},$$
(5)

where  $j, k = 1, 2, x_1 \equiv x, x_2 \equiv y$ , and the Einstein's convention is adopted, i.e., automatic summation over repeating indices (k, in this case). If identity (5) is substituted in Eq. (4), the integral of the first (full-derivative) term vanishes, in both cases of the infinite area and the one constrained by BC (2) (in the latter case, the result of the integration of the full derivative, which amounts to the *surface term* taken at the edge of the square, is zero pursuant to BC (2)). The substitution of the second term from expression (5) in Eq. (4) yields zero too, as this term is imaginary. Thus, Eq. (4) is reduced to the form with the right-hand side (RHS) determined by the third term from the RHS of Eq. (identity):

$$\frac{d\mathbf{R}}{dt} = \frac{i}{2N} \int \int \psi \nabla \psi^* dx dy + \text{c.c.}$$
 (6)

To continue the derivation of the (amended) ET, expression (6) is repeatedly differentiated with respect to t, again substituting  $\partial \psi/\partial t$  as per Eq. (1). After straightforward manipulations similar to those outlined above (which include the integration by parts and dropping the surface terms which are nullified by BC (2)), an intermediate result is

$$\frac{d^2\mathbf{R}}{dt^2} = \frac{1}{N} \int \int \left[ -\frac{1}{2} \nabla^2 \psi + U(r)\psi + g|\psi|^2 \psi \right] \nabla \psi^* dx dy + \text{c.c.}$$
 (7)

Further consideration easily shows that the term  $\sim g$  in Eq. (7) yields zero contribution, the term  $\sim U$  yields, with the help of the integration by parts, precisely the quantum-mean (qmean, alias expectation) value of the potential force,

$$-\left(\nabla U(R)\right)_{\text{qmean}} \equiv -\frac{1}{N} \int \int \nabla U(r) \left|\psi\left(x,y\right)\right|^2 dx dy, \tag{8}$$

and there remains an additional "anomalous" integro-gradient term in the resulting expression for the COM's acceleration, which originates from the quantum-pressure term  $-\frac{1}{2}\nabla^2\psi$  in the integrand on the RHS of Eq. (7):

$$\frac{d^2 \mathbf{R}}{dt^2} = -\left(\nabla U(R)\right)_{\text{qmean}} - \frac{1}{2N} \left[ \int \int \nabla^2 \psi^* \cdot \nabla \psi dx dy + \text{c.c.} \right]. \tag{9}$$

Writing the integrand of the second term on the right-hand side of Eq. (9) with the explicit coordinate indices (cf. Eq. (5)), it is easy to represent it in the form of a full derivative:

$$-\frac{1}{2N} \left( \partial_j \psi \cdot \partial_{kk}^2 \psi^* + \partial_j \psi^* \cdot \partial_{kk}^2 \psi \right) \equiv \frac{1}{2N} \left[ -\partial_k \left( \partial_j \psi \cdot \partial_k \psi^* + \partial_j \psi^* \cdot \partial_k \psi \right) + \partial_j \left( \partial_k \psi^* \cdot \partial_k \psi \right) \right], \tag{10}$$

In the case of a localized wave function in the infinite area, the integral of the full-derivative term (10) immediately vanishes, reducing Eq. (9) to the usual ET form:

$$\frac{d^2 \mathbf{R}}{dt^2} = -\left(\nabla U(R)\right)_{\text{qmean}}.\tag{11}$$

In particular, if  $\psi(x,y)$  is highly localized,  $(\nabla U(R))_{\text{qmean}}$  may be approximated at  $\nabla U(R)$ , producing the Newton's equation of motion from classical mechanics.

A well-known example is Eq. (1) in the infinite area with the harmonic-oscillator (HO) trapping potential (in the scaled form),

$$U_{\text{HO}} = (1/2)(x^2 + y^2). \tag{12}$$

In that case, the last term in Eq. (9) vanishes, as said above, while the remaining form of Eq. (9) is fully identical to the classical equation of motion,

$$\frac{d^2\mathbf{R}}{dt^2} = -\mathbf{R} \tag{13}$$

because

$$-\frac{1}{N} \int \int \nabla U(r) |\psi(x,y)|^2 dx dy = -\frac{1}{N} \int \int \mathbf{r} |\psi(x,y)|^2 dx dy = -\mathbf{R}.$$

On the other hand, in the case of the infinitely deep box with U = 0, defined by BC (2), the entire effective force in the COM equation of motion (9) is produced by the "anomalous" term, which may be construed as the result of the interaction of the trapped condensate with the edges of the potential box. Indeed, the integration of the full-derivative term in Eq. (9), with U = 0 (no potential acting inside the box) casts the COM equation of motion in the following form, with rather cumbersome expressions for the components of the edge-exerted force:

$$\frac{d^{2}X}{dt^{2}} = \frac{1}{N} \left[ \frac{1}{2} \int_{-L/2}^{+L/2} \left( \left| \partial_{y} \psi \right|^{2} - \left| \partial_{x} \psi \right|^{2} \right) dy \Big|_{x=-L/2}^{x=+L/2} - \int_{-L/2}^{+L/2} \operatorname{Re} \left( \partial_{x} \psi \cdot \partial_{y} \psi^{*} \right) dx \Big|_{y=-L/2}^{y=+L/2} \right] \equiv F_{x}, \tag{14}$$

$$\frac{d^{2}Y}{dt^{2}} = \frac{1}{N} \left[ \frac{1}{2} \int_{-L/2}^{+L/2} \left( \left| \partial_{x} \psi \right|^{2} - \left| \partial_{y} \psi \right|^{2} \right) dx \Big|_{y=-L/2}^{y=+L/2} - \int_{-L/2}^{+L/2} \operatorname{Re} \left( \partial_{y} \psi \cdot \partial_{x} \psi^{*} \right) dy \Big|_{x=-L/2}^{x=+L/2} \right] \equiv F_{y}, \tag{15}$$

where  $\begin{vmatrix} x,y=\pm L/2 \\ x,y=-L/2 \end{vmatrix}$  implies, as usual, taking the difference of the expression at points  $x,y=\pm L/2$ . Similar expressions can be derived for 2D potential boxes of different shapes, such as a cylindrical one.

In the case of the 1D infinitely deep box, the integration in the 1D version of Eq. (9) (with U = 0) can be easily performed, leading to the following COM equation of motion:

$$\frac{d^2X}{dt^2} = \frac{1}{2N} \left| \partial_x \psi \right|^2 \Big|_{x=-L/2}^{x=+L/2} \equiv F_{1D}. \tag{16}$$

On the other hand, the "anomalous" force does not appear in the 1D ring-shaped setup, which is modeled by the 1D GPE subject to the periodic BC.

A relevant generalization of the underlying GPE (1) is the one in which the nonlinearity coefficient g may be spatially dependent, g(x,y) [27]. Because g does not explicitly appear in Eqs. (14), (15) and (16), these equations remain valid in this case too.

# III. NUMERICAL RESULTS

# A. The 2D system

First, we provide typical examples of the COM motion in the framework of the 2D GPE (1) which includes the HO trapping potential (12) and the self-defocusing, zero, or focusing nonlinearity, corresponding to g = +1,0 or -1, respectively. The initial condition is taken as a linear combination of the ground state and lowest vortex eigenmode of the 2D linear HO (the one with g = 0) [3], with the ratio of the real participation coefficients 1: a, i.e.,

$$\psi_0(x,y) = \aleph \exp\left(-\frac{1}{2}(x^2 + y^2)\right) [1 + a(x+iy)],$$
 (17)

where  $\aleph$  is a real amplitude. The 2D norm of input (17) is

$$N = \pi \aleph^2 \left( 1 + a^2 \right), \tag{18}$$

At point

$$x = x_p \equiv \frac{\sqrt{1 + 4a^2 - 1}}{2a}, \ y = 0,$$
 (19)

the input (17) attains its maximum (peak) value,

$$A_p = \aleph \exp\left(-x_p^2/2\right) \left(1 + ax_p\right). \tag{20}$$

The COM coordinates (3) of input (17) are

$$X = a/(1+a^2) \equiv x_{\text{COM}}, Y = 0.$$
 (21)

Obviously, the linear Schrödinger equation with input (17) produces an elementary solution for the wave function,

$$\psi(x, y; t) = \aleph \exp\left(-\frac{1}{2}(x^2 + y^2)\right) \left[e^{-it} + a(x + iy)e^{-2it}\right].$$
 (22)

In the course of the evolution governed by this solution, the peak-value point moves with angular frequency  $\omega = 1$  along the ring  $\sqrt{x^2 + y^2} = x_p$ , keeping the constant peak value (20) of  $|\psi(x, y, t)|$ .

Characteristic examples of the evolution of the input (17) for the three above-mentioned cases, g = +1, 0, and -1, are displayed in Fig. 1, for the fixed values of the norm, N = 5.7, and a = 2 in Eq. (17) (hence, the amplitude is  $\aleph \approx 0.60$ , and the peak value is  $A_p \approx 1.14$ , according to Eqs. (19) and (20)). The simulations were performed in the square of size  $L \times L = 12 \times 12$ , by means of the split-step Fourier method based on a set of  $256 \times 256$  modes.

In full agreement with the normal ET, it is observed that, while the evolution of the wave function as a whole is quite different in the cases of the self-repulsion, no self-interaction, and self-attraction (as specified, in particular, by the evolution of the peak value displayed in Fig. 1(a)), the evolution of the COM coordinates X(t) and Y(t) is identical in all the cases, given by an obvious solution of Eq. (13):

$$X(t) = x_{\text{COM}} \cos t, \ Y(t) = x_{\text{COM}} \sin t, \tag{23}$$

with  $x_{\text{COM}}$  defined by Eq. (21). The corresponding COM trajectory in the (x,y) plane is the ring of radius  $x_{\text{COM}}$ . Note that the 2D GPE with g=-1 may give rise to the wave collapse (catastrophic self-compression of the wave function) [23–25] if the input's norm exceeds the well-known critical value,  $N_{\text{cr}} \approx 5.85$  (in the present notation; its approximate variational value is  $(N_{\text{cr}})_{\text{var}} = 2\pi$  [26]). The proximity of N=5.7 to  $N_{\text{cr}}$  leads to irregular large-amplitude oscillations of  $A_p(t)$  in Fig. 1(a) and irregular spatiotemporal evolution in Fig. 1(b); nevertheless, this irregularity produces no effect on the ET-supported strictly harmonic oscillations of the COM coordinates in Fig. 1(c). Furthermore, additional simulations of the collapse development in the case of the input with  $N>N_{\text{cr}}$  (not shown here in detail) corroborate that the strictly harmonic oscillations of X(t) and Y(t) persist even in this case, as long as the appearance of very large amplitudes, generated by the collapse, does not break the simulation algorithm.

The central point of the present work is to consider the dynamics governed by the GPE in the 2D potential box with U = 0, subject to BC (2), for which the ET takes the amended form given by Eqs. (9) or (14) and (15). A set of characteristic examples is displayed in Fig. 2, taking the initial condition as a superposition of obvious eigenstates of the 2D linear Schrödinger equation with BC (2),

$$\psi_0(x,y) = \Re\{\cos(kx)\cos(ky) + a\left[\sin(2kx)\cos(ky) + i\cos(kx)\sin(2ky)\right]\},\tag{24}$$

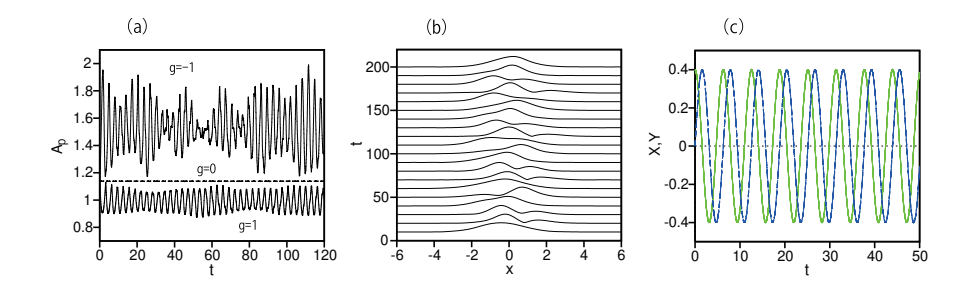


FIG. 1. (a) The evolution of the peak (largest) value of  $|\psi(x,y,t)|$  for g=-1 (the upper solid line), g=0 (the flat dashed line), and g=+1 (the lower solid line), as produced by the numerical simulations of Eq. (1) with the HO potential (12) and input (17). (b) The evolution of  $|\psi(x,y,t)|$  in the cross section y=0 for g=-1. (c) The evolution of the COM coordinates X and Y (the solid green and dashed blue lines, respectively), as produced by the data of the numerical simulations, as per definitions (3) for g=+1, 0, and -1. The ET-predicted dependences (23) of the COM coordinates are plotted by the solid green and dashed blue lines, respectively. The parameters of the input (17) are N=5.7 and a=2, hence the other parameters are  $\aleph\approx0.60$ ,  $A_P\approx1.14$ , and  $x_{\rm COM}=0.4$ , see Eqs. (18), (20), and (21).

where  $k = \pi/L$ , and the amplitude is matched to a given value of the 2D norm,  $\aleph = \sqrt{4N/[L^2(1+2a^2)]}$ . This input is roughly similar to the above one (17), with the first term representing the ground state of the linear system, and the second one, with the real relative-participation amplitude a, emulating the vortex term in Eq. (17). Characteristic examples, produced by the numerical simulations of Eq. (1) with U=0, BC (2), and input (24), are presented in Fig. 2 for norm N=5 and relative participation amplitude a=0.4 in expression (24) (in particular, the dynamics displayed in panel (c) does not lead to the collapse in the case of the self-focusing, as N=5 is smaller than the above-mentioned critical value,  $N_{\rm cr} \approx 5.85$ ).

The solution of the linear version of Eq. (1), with U = g = 0 and BC (2), produced by input (24), is obvious:

$$\psi(x,y,t) = \Re\left\{\cos(kx)\cos(ky)e^{-i\omega_1t} + a\left[\sin(2kx)\cos(ky)e^{-i\omega_2t} + ia\cos(kx)\sin(2ky)\right]e^{-i\omega_2t}\right\},\tag{25}$$

with eigenfrequencies  $\omega_1 = k^2$  and  $\omega_2 = 5k^2/2$ . In this case, the components of the effective edge-exerted force in the 2D potential box, defined by the second term on the right-hand side of Eq. (9), or, alternatively, by the more explicit expressions (14) and (15), are readily calculated as

$$F_x = -\frac{8\pi^2 a}{L^3 (1 + 2a^2)} \cos((\omega_2 - \omega_1)t), \ F_y = -\frac{8\pi^2 a}{L^3 (1 + 2a^2)} \sin((\omega_2 - \omega_1)t).$$
 (26)

In the framework of the nonlinear GPE, with  $g = \pm 1$ , it is necessary to obtain numerical solutions of Eq. (1) and then compute the effective force, substituting the numerical solutions in Eq. (9) or Eqs. (14) and (15).

For the GPE in the 2D potential box with the self-defocusing (g = +1) and focusing (g = -1) nonlinearities, as well as for the linear GPE (with g = 0), Figs. 2(a), (c), and (b) display, severally, the evolution of the COM coordinates X and Y (the green solid and blue dashed lines, respectively), as directly obtained from the numerical simulations. The X(t) and Y(t) dependences are indistinguishable from their counterparts produced by the amended ET, i.e., Eq. (9) or Eqs. (14) and (15), thus corroborating the amended ET for the 2D potential box in both the linear and nonlinear cases. Note that, unlike the usual ET (cf. Fig. 1), the amended version predicts irregular (apparently chaotic) COM motion in the strongly nonlinear setup. The chaotic character of the motion under the action of the nonlinearity  $(g \neq 0)$  is corroborated by positive values of the respective Lyapunov exponents. The largest exponents are numerically evaluated as  $2.0 \times 10^{-3}$  at g = +1,  $-1.5 \times 10^{-7}$  at g = 0, and  $1.9 \times 10^{-3}$  at g = -1.

# B. Reduction to the 1D potential box

The underlying 2D GPE (1) with U = 0, subject to BC (2), can be reduced to the 1D form by considering a narrow potential box, of size (L, l) in the x and y directions, with  $l \ll L$ , taking the limit of  $l \to 0$ , and performing integration in the y direction. Thus one arrives at the 1D version of Eq. (9),

$$i\frac{\partial\psi}{\partial t} = -\frac{1}{2}\frac{\partial^2\psi}{\partial x^2} + g|\psi|^2\psi,\tag{27}$$

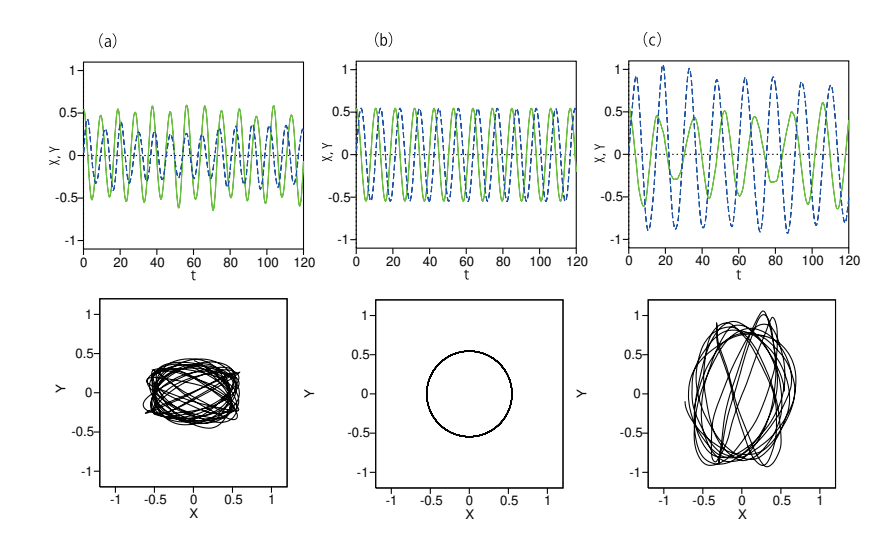


FIG. 2. The evolution of the COM coordinates X(t) and Y(t) (the solid green and dashed blue lines, respectively), as directly produced by the simulations of the 2D GPE (1) with U=0, BC (2), and input (24). These dependences are indistingushable from their counterparts produced by the equations of motion (14) and (15), which represent the amended ET for the 2D potential box. Panels (a), (b), and (c) represent, severally, the GPE with g=+1, g=0, and g=-1. The corresponding COM trajectories in the (x,y) plane are plotted in bottom panels. The parameters are N=5, a=0.4, and L=10.

with BC  $\psi(x = \pm L/2) = 0$  and the nonlinearity coefficient set, as above, to be  $g = \pm 1$  or 0. In this connection, it is relevant to mention analytical stationary equations of Eq. (27) with this BC, which were found for g = +1 [28] and g = -1 [29].

Here we display the results for the fixed norm  $N = \int_{-L/2}^{+L/2} |\psi(x)|^2 dx = 5$  and the 1D-box size L = 4. The initial condition is chosen as a mixture of the ground and first excited states, roughly similar to the 2D inputs (17) and (24):

$$\psi_0(x) = \Re\left[\cos(\pi x/L) + a\sin(2\pi x/L)\right],\tag{28}$$

with the amplitude expressed in terms of the norm as  $\aleph = \sqrt{2N/[L(1+a^2)]}$ . In the case of g = 0, the solution to Eq. (27) with input (28) is obvious:

$$\psi(x,t) = \aleph \left[ \cos(\pi x/L) e^{-i\omega t} + a \sin(2\pi x/L) e^{-4i\omega} \right],$$

with  $\omega = \pi^2/(2L^2)$ , the corresponding effective edge-generated force (16) being

$$F_{1D} = -\frac{8\pi^2 a}{L^3 (1+a^2)} \cos(3\omega t), \qquad (29)$$

cf. Eq. (26).

The results are given here for the relative participation coefficient of the first excited state a=0.2 in Eq. (28), hence  $\aleph \approx 1.57$ . The simulations were performed by means of the split-step Fourier method with 512 modes. Solid curves in Figs. 3(a), (b), and (c) display the evolution of the COM coordinate,  $X(t) = N^{-1} \int_{-L/2}^{+L/2} x |\psi(x,t)|^2 dx$  (solid lines), for g=+1, 0, and -1, respectively, as directly computed from the data of the simulations of Eq. (27). In the same figures, the dashed curves, which are actually indistinguishable from the solid ones, represent the COM coordinate,  $X_r(t)$ , as obtained from Eq. (16). Thus, the amended ET is fully corroborated in the 1D case too.

#### IV. CONCLUSION

The usual form of the ET (Ehrenfest theorem), which was established about 100 years ago [1], states that the motion of the COM (center of mass) of the 1D quantum-mechanical wave packet is governed by the corresponding classical equation of motion, in which the usual force is replaced by its expectation quantum-mechanical value (it is identical to the classical force in the case of the HO (harmonic-oscillator) potential). More recently, it has been found that ET is not valid, in this form, for the quantum-mechanical particle trapped in the infinitely deep 1D potential

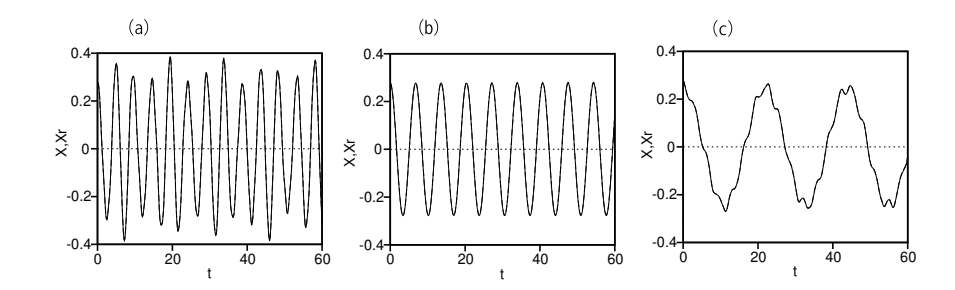


FIG. 3. The evolution of the COM coordinate X (the solid line), as produced by the direct simulations of Eq. (27) with input (28) in the 1D potential box, and its counterpart  $X_r$  (the dashed line), as reconstructed by means of the amended-ET equation (16), for g = +1 (a), g = 0 (b), and g = -1 (c).

box. An alternative form of the ET was derived for this case, with an effective force induced by the interaction of the particle with the edges of the 1D box. In the present work, we have extended the concept of the amended ET for the linear Schrödinger equation replaced by the nonlinear GPE (Gross-Pitaevskii equation) with the cubic self-focusing or defocusing term, as well as for the 2D potential box. In the latter case, we have derived an effective force induced by edges of the square-shaped box, while the nonlinearity does not add a direct contribution to the ET, in the 1D and 2D cases alike. Nevertheless, the nonlinearity affects the amended ET through the edge-generated force. In particular, the presence of the nonlinear terms in the underlying GPE can make the COM motion in the potential box irregular (chaotic). The validity of the amended ET in both the 1D and 2D settings is fully corroborated by the comparison with results of the full numerical simulations. These results are directly relevant to the current experiments with atomic BEC trapped in rectangular potential boxes.

As an extension of the analysis, it may be interesting to develop it for a system of nonlinearly coupled GPEs modeling a binary BEC [30]. Such a generalization may be straightforward, as the above-mentioned equations (14), (15) and (16) will not include terms accounting for the interaction between the two components, hence the equations will keep their form separately for each component. Another relevant possibility is to consider a 2D cylindrical potential box, as well as a 3D one of the cubic form, as the trapping potentials of these types are also available to the experiment. On the other hand, a challenging possibility may be to introduce an amended ET in relativistic quantum mechanics, cf. Refs. [31–33].

- [1] P. Ehrenfest, Bemerkung über die angenäherte Gültigkeit der klassischen Mechanik innerhalb der Quantenmechanik, Zeitschrift für Physik 45, 455-457 (1927).
- [2] A. E. Ruark, The Zeeman Effect and Stark Effect of Hydrogen in Wave Mechanics; The Force Equation and the Virial Theorem in Wave Mechanics, Phys. Rev. 31, 533-538 (1928).
- [3] L. D. Landau and E. M. Lifshitz, Quantum Mechanics (Nauka publishers, Moscow, 1974).
- [4] D. Bohm, Quantum Theory (Dover, New York, 1989.
- [5] L. E. Ballentine, Quantum Mechanics (World Scientific, Singapore, 2000).
- [6] D. S. Rokhsar, Ehrenfest's theorem and the particle-in-a-box, Am. J. Phys. 64, 1416-1418 (1996).
- [7] V. Alonzo, S. De Vincenzo, and L. A. González-Díaz, On the Ehrenfest theorem in a one-dimensional box, Nuvo Cim. 115B, 155-164 (2000).
- [8] S. De Vincenzo, Confinement, average forces, and the Ehrenfest theorem for a one-dimensional particle, Pramana J. Phys. 80, 797-810 (2013).
- [9] I. Albrecht, J. Herrmann, A. Mariani, U.-J. Wiese, and V. Wyss, Bouncing wave packets, Ehrenfest theorem, and uncertainty relation based upon a new concept for the momentum of a particle in a box, Annals of Physics **452**, 169289 (2023).
- [10] D. Giordano and P. Amodio, Considerations about the incompleteness of the Ehrenfest's theorem in quantum mechanics, Eur. J. Phys. 42 065405 (2021).
- [11] K. S. Gupta and S. G. Rajeev, Renormalization in quantum mechanics, Phys. Rev. D 48, 5940-5945 (1993).
- [12] L. P. Pitaevskii and A. Rosch, Breathing modes and hidden symmetry of trapped atoms in two dimensions, Phys. Rev. A 55, R853-R856 (1997).
- [13] H. E. Camblong, L. N. Epele, H. Fanchiotti, and C. A. García Canal, Renormalization of the Inverse Square Potential, Phys. Rev. Lett. 85, 1590-1593 (2000).
- [14] H. E. Camblong, L. N. Epele, H. Fanchiotti, and C. A. García Canal, Dimensional Transmutation and Dimensional Regularization in Quantum Mechanics: II. Rotational Invariance, Annals of Physics 287, 57-100 (2001).

- [15] K. Fujikawa, Quantum anomaly and geometric phase: Their basic differences, Phys. Rev. D 73, 025017 (2006).
- [16] M. Olshanii, H. Perrin, and V. Lorent, Example of a Quantum Anomaly in the Physics of Ultracold Gases, Phys. Rev. Lett. 105, 095302 (2010).
- [17] H. Sakaguchi and B. A. Malomed, Suppression of the quantum-mechanical collapse by repulsive interactions in a quantum gas, Phys. Rev. A 83, 013607 (2011).
- [18] T. P. Meyrath, F. Schreck, J. L. Hanssen, C. S. Chuu, and M. G. Raizen, Bose-Einstein condensate in a box, Phys. Rev. A 71, 041604 (2005).
- [19] A. L. Gaunt, T. F. Schmidutz, I. Gotlibovych, R. P. Smith, and Z. Hadzibabic, Bose-Einstein Condensation of Atoms in a Uniform Potential, Phys. Rev. Lett. 110, 200406 (2013).
- [20] C. Eigen, A. L. Gaunt, A. Suleymanzade, N. Navon, Z. Hadzibabic, and R. P. Smith, Observation of Weak Collapse in a Bose-Einstein Condensate, Phys. Rev. X 6, 041058 (2016).
- [21] N. Navon, R. P. Smith, and Z. Hadzibabic, Quantum gases in optical boxes, Nature Phys. 17, 1334-1341 (2021).
- [22] L. E. Young-S and S. K. Adhikari, Supersolid-like square- and triangular-lattice crystallization of dipolar droplets in a box trap, Eur. Phys. J. Plus 137, 1153 (2022).
- [23] L. Bergé, Wave collapse in physics: principles and applications to light and plasma waves, Phys. Rep. 303, 259-370 (1998).
- [24] E. A. Kuznetsov and F. Dias, Bifurcations of solitons and their stability, Phys. Rep. 507, 43-105 (2011).
- [25] G. Fibich, The Nonlinear Schrödinger Equation: Singular Solutions and Optical Collapse (Springer, Heidelberg, 2015).
- [26] M. Desaix, D. Anderson, and M. Lisak, Variational approach to collapse of optical pulses, J. Opt. Soc. Am. B 8, 2082-2086 (1991).
- [27] D.-S. Wang, X.-H. Hu, J. Hu, and W. M. Liu, Quantized quasi-two-dimensional Bose-Einstein condensates with spatially modulated nonlinearity, Phys. Rev. A 81, 025604 (2010).
- [28] L. D. Carr, C. W. Clark, and W. P. Reinhardt, Stationary solutions of the one-dimensional nonlinear Schrödinger equation. I. Case of repulsive nonlinearity, Phys. Rev. A 62, 063610 (2000).
- [29] L. D. Carr, C. W. Clark, and W. P. Reinhardt, Stationary solutions of the one-dimensional nonlinear Schrödinger equation. II. Case of attractive nonlinearity, Phys. Rev. A 62, 063611 (2000).
- [30] D.-S. Wang, X.-H. Hu, and W. M. Liu, Localized nonlinear matter waves in two-component Bose-Einstein condensates with time- and space-modulated nonlinearities, Phys. Rev. A 82, 023612 (2010).
- [31] V. Alonso and S. De Vincenzo, Ehrenfest-type theorems for a one-dimensional Dirac particle, Physica Scripta 61, 396-400 (2000).
- [32] İ. Bialynicki-Birula and Z. Bialynicka-Birula, Helical beams of electrons in a magnetic field: new analytic solutions of the Schrödinger and Dirac equations, J. Phys. A: Math. Theor. **56**, 285302 (2023).
- [33] L. Chataignier, Phase time and Ehrenfest's theorem in relativistic quantum mechanics, Phys. Rev. D 110, 126023 (2024).